The 2016 World Congress on
Advances in Civil, Environmental, and Materials Research (ACEM16)
Jeju Island, Korea, August 28-September 1, 2016

Hybrid Core/Shell Nanostructures: Response towards Structural and Morphological properties

*U. Khan,[a] N. Adeela,[b] S. Riaz,[b] and S. Naseem[b]

[a]*Beijing National Laboratory for Condensed Matter Physics, Institute of Physics,Chinese Academy of Sciences, Beijing 100190, China. E-mail: usman_cssp@yahoo.com.*

[b]*Centre for Solid State Physics, university of the Punjab, Lahore, Pakistan.*

ABSTRACT: The versatile approach towards nanofabrication of highly reproduceable Co/$BiCoO_3$ (Co/BCO) Core/Shell (CS) nanowires (NWs) with different diameters has been adopted by demonstrating easily available and low cost sol-gel and electrodepostion route. X-ray diffraction (XRD) analysis confirmed tetragonal system of BCO nanoshells (NSs) with space group of *P4mm*. Scanning electron microscopy (SEM) clearly demonstrates uniform morphology with well alligned CS NWs.

INTRODUCTION

Magnetic nanostructures have attracted renewed interest over their respective bulk counterparts for the synthesis of highly ordered arrays embedded into the nano-channels of aluminum oxide templates (Masuda et.al., 1995). One dimensional (1D) nanogeometry, previously, has been intensively utilized because of its potential technological applications mainly interconnection for advance magnetic storage devices, magnetic sensors, magnetic

memory and microwave devices (Gapin et.al., 2006 and Parkin et.al., 2008). Among several nanostructures, limited research has been recorded for the demonstration of Core/Shell (CS) nanostructures, especially CS nanowires (NWs). Magnetic CS NWs have been given considerable attention during the last few decades due to their remarkable characteristics like, magnetic anisotropy, magnetization reversal process, thermal stability and exchange bias (over their respective simple NWs) (Chaudhri et.al., 2012 and Zeng et.al., 2004). Three different modes of magnetization reversal process (MRP) has been identified in NWs as a function of its geometrical parameters (Landeros et. Al., 2007). These modes are characterized as coherent mode (C-mode) in which spins simultaneously rotate; transverse mode (T-mode) with spins flip progressively as function of transverse domain wall and vortex domain wall dependent spins inversion is discussed in third kind of reversal process called vortex mode (V-mode). In extension, if diameter of NWs is less than its critical value then it is referred to C/T-mode and diameter greater than critical value is expected to V-mode (Zeng et.al., 2002). CS NWs, with core as ferromagnetic/antiferromagnetic (FM/AFM) and nanoshell as AFM/FM, respectively, have possibility to generate interesting phenomenon of magnetic exchange bias (EB). One of the possible reasons to have great impact on the exchange bias is the thickness of ferromagnetic layer and there is the inverse relation between thickness of ferromagnetic layer and exchange bias according to the equation $H_{ex} = J/Mt$ with J is the interlayer exchange coupling between ferromagnetic and antiferromagnetic layer and , M & t stands for magnetization & thickness of FM layer, respectively (Meiklejohn et.al., 1962 and

Nogues et.al., 1999). EB is not only important in 1D geometry but also in 0D (CS nanoparticles) and 2D geometry (thin films) due to its potential response towards spin valve and magnetic tunnel junction's fabrication (Sort et.al., 2004 and Moodera et.al., 1999). The objective of present article is to study the fabrication of highly ordered ferromagnetic/multiferroic CS NWs as a function of different diameters. Metallic cobalt (Co) and perovskite $BiCoO_3$ (BCO) are utilized as nanocore and nanoshell in coaxial nanogeometry, respectively. We focus on morphological parameters to improve Core/Shell nanogeometry.

Antiferromagnetic nanoshell of BCO was fabricated with chemical salts/solutions containing Bismuth (III) Nitrate [$Bi(NO_3)_3$; Alfa Aesar, >98%], Cobalt (III) Nitrate [$Co(NO_3)_3$; Alfa Aesar, >98%] and Ethylene Glycol [$C_3H_8O_2$; Alfa Aesar, >99%]. The precursors objected for metallic Co as core were Cobalt (II) Sulfate [$CoSO_4$; Alfa Aesar, >98%], and boric acid [H_3BO_3; Alfa Aesar, >98%). Well-ordered anodic Alumina nanomembranes/templates (AAO) were fabricated by two step electrochemical route with pore-diameters of 100 nm, 150nm & 200nm and nominal thickness of 40 µm each. The pore-density of AAO nanomembranes is explained in detail in supplementary data.

BCO nanoshell was fabricated by low cost and easily available sol-gel route. Nanoshell of BCO evolved four basic steps involving, sol optimization, gel formation and densification followed by drying process. A typical fabrication route is described as follows; Bismuth Nitrate and Cobalt Nitrate with stoichiometric molar ratio were mixed in Ethylene Glycol under continuous electromagnetic stirring at room temperature for 6 h. In order to avoid impurity phases and maintain pH of solution, 3 microliters of Nitric acid was added in

product and stirred until the gel formation. AAO nanomembranes of different pore-diameters d=100nm, 150nm and 200nm were divided into small pieces (1cm x 1cm) and heated at 300 ℃ prior to dipping process. The unstressed, uniform and smooth nanomembranes were selected for further process. Thickness of AFM materials (BCO) for CS nanostructures with hybrid FM/AFM interface is crucial parameter. Presently, we have adopted different techniques to increase the thickness of BCO NSs embedded inside AAO template and observed that thickness of NSs can be increased if one side of template is sputtered prior to sol-gel process. The detailed logics are explained well in supplementary data. Later on, one side of the treated nanomembranes were sputtered with Cu, 5nm and emerged in final product at room temperature for 20min.

Gel-coated nanomembranes were dried initially at 300℃ and densified at 500℃ with 1℃/min for 6 h in vacuum to get nanoshell of BCO embedded in it. Afterwards, metallic Co was electrodeposited inside BCO nanoshell in order to construct CS nanogeometry with different pore-diameters. The importance for sputtering of seed layer prior to fabricate BCO nanoshell embedded in AAO nanomembrane and fabrication procedure for electrodeposited Co NWs as nanocore are discussed in supplementary data. The detailed CS (Co/BCO) fabrication process is explained in Fig. 1.

Structurally the samples were analyzed with X-ray diffraction machine by using Cu Kα with wavelength of λ = 0.154056 nm (XRD: RIGAKU-D/MAX-2400). Detailed morphology of CS NWs was characterized by field emission scanning electron microsope (FE-SEM: Hitachi S-4800) equipped with detector for energy dispersive X-ray spectroscopy (EDS). The

ferroelectric characteristics of nanotubes were studied by ferroelectric tester (Radiant; Premier II).

RESULTS AND DISCUSSION

XRD patterns for BCO nanoshells and Co/BCO CS NWs achieved at room temperature are presented in Fig. 2a. Crystal structure of BCO nanoshells annealed at 500℃ is demonstrated tetragonal system with space group of *P4mm*. Crystallographic Bragg's peaks located at 2θ = 20.71°, 30.12°, 36.22° and 70.22° correspond to (100), (110), (111) and (310) planes, respectively. It has been observed that XRD data of nanoshells matches well with already reported research work (Sun et.al., 2014). The pattern also shows the absence of any obvious impurity phases in the fabricated nanoshells and broader peaks are attributed to small crystallite dimensions. The results analogous to present work have already been published in literature for the case of solgel treated nanotubes (Javed et.al., 2015). The BCO nanoshells were further investigated with elemental analysis and only the presence of Co, Bi and O has been confirmed without other impurity elements (Fig. 2b).

The morphology of BCO nanoshells with 100nm of pore-diameter taken by SEM is represented in Fig. 3a. Herein, it is worth to mention that at higher temperature Al_2O_3 (nanomembranes) start reacting with solgel coated nanomaterials, which in present case is limited to 500℃ in order to make sure Al_2O_3 is not reacting with nanoshell geometry. Later on, metallic Co NWs were deposited inside BCO nanoshells via electrodeposition method to investigate magnetic properties of CS Co/BCO NWs. XRD results of Co NWs embedded in BCO nanoshells are shown in Fig. 2. Bragg's peaks reflected from (100),

(002) and (101) planes are located at 2θ = 41.68°, 44.76° and 47.57°, respectively and correspond to hexagonal crystal structure. The behavior of embedded NWs is similar with JCPDS (PDF-2 / Release 2012, RDB 05-727). Moreover, nanoshells with 100nm of diameter are presented here for crystal structure and elemental analysis. Rietveld refinement is a well- established process to explore structural details using powder diffraction data. In the very first step of refinement, background and scale factors were refined. Fitting quality of experimental data is induced by computing goodness of fit and two reliability factors, profile factor (Rp) and weighted profile (Rwp) which must be close to or less than 10%). The best fit to experimental data is achieved when these factors reach their minimum values. Then, structure is considered as satisfactory and the parameters are mentioned in table S1.

The morphology of CS NWs clicked by SEM is shown in Fig. 3. The pore-diameter and length of nanoshells depend on AAO nanomembranes. Thickness of nanoshells (antiferromagnetic materials) in CS NWs has great impact on magnetic properties.[41] In present study, three different pore-diameters 100nm, 150nm and 200nm are used to analyze diameter dependent magnetic properties of CS NWs. BCO wall thickness of ~25nm was fixed against each diameter which results, in comparison, large size of nanocores as diameter increases to 150nm and 200nm. It can be observed with SEM micrographs that morphology of CS nanostructures is quiet homogeneous, dense and clean with aligned NWs. It is important to describe the factors involving for better morphology includes etching; chemicals, time, and temperature which in detail are mentioned in supplementary data.

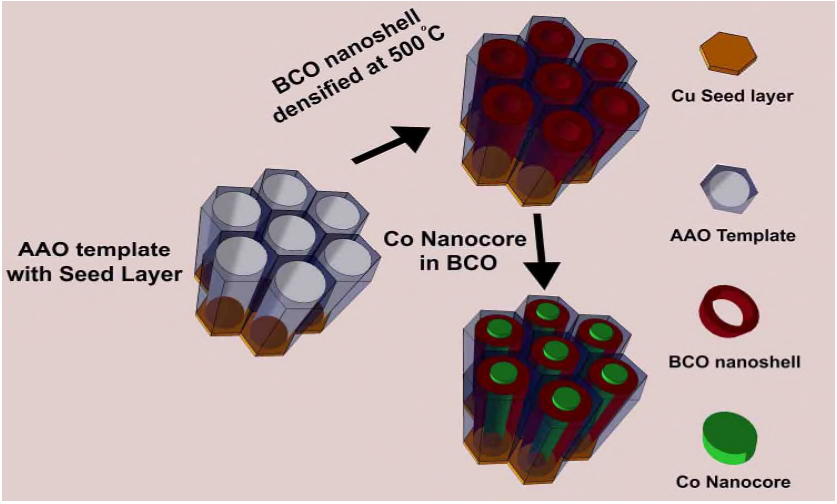

Fig. 1 Complete fabrication procedure for Co/BCO CS NWs embedded in alumina membranes

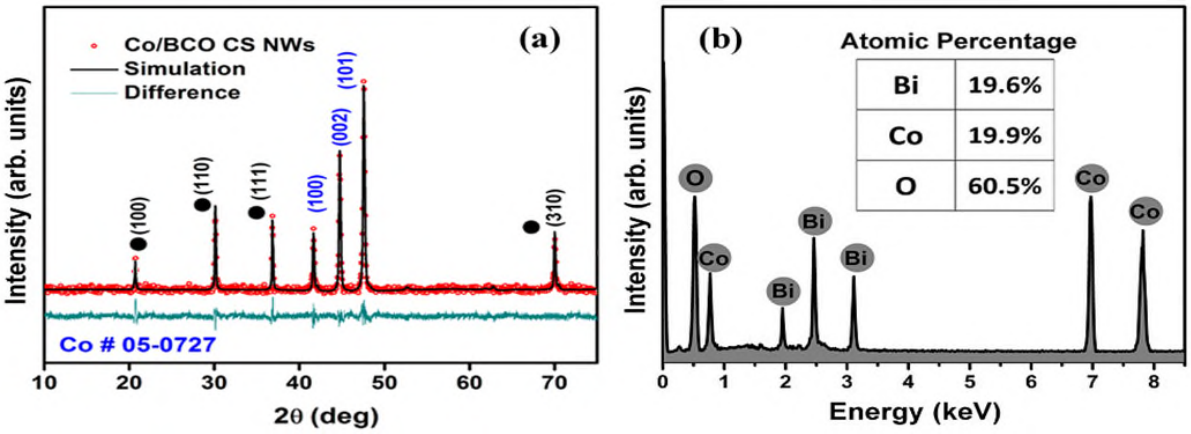

Fig. 2 (a) Structural analysis by X-ray powder diffraction (XRD) of Core/shell (CS) Co/BCO NWs (NWs). While XRD of BCO nanoshells (NSs) is shown in the inset (a) and energy

dispersive X-ray spectra (EDS) of BCO NSs embedded in AAO templates is represented in (b).

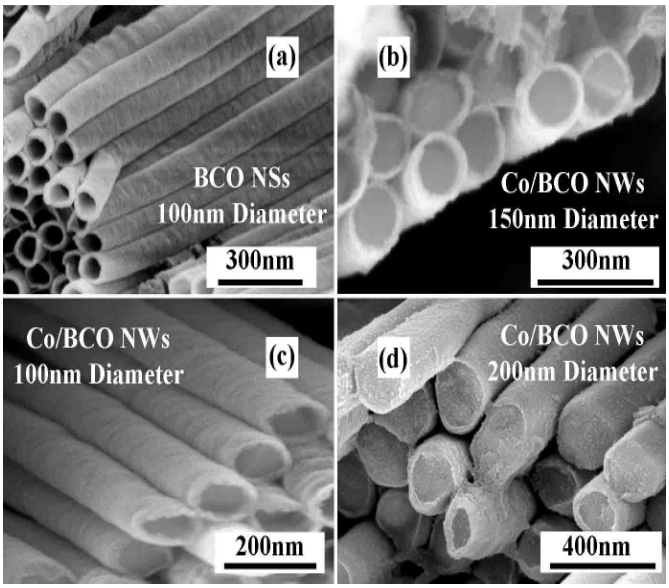

Fig. 3 (a) Scanning electron microscope (SEM) image for BCO NSs with 100nm of diameter (b) SEM micrograph for Co/BCO NWs with 100nm, 150nm and 200nm of diameter are shown in (b-d), respectively.

Conclusions

In remarks, we have established CS NWs consisting of Co as ferromagnetic Core and BCO antiferromagnetic Shell embedded in alumina templates (AAO) with varying diameter. To control the wall thickness of BCO in AAO template was difficult task which was ended with ~25nm via solgel route, detail description is given in supplementary data. Polarization verses electric field loop announced for multiferroic behavior of BCO NSs. Afterwards, better morphology and PE response of BCO led us to electrodeposit Co NWs into BCO

nanochannels that were previously embedded inside AAO template. Structural analysis confirmed tetragonal system with *P4mm* space group for BCO NSs and hexagonal crystal structure for Co NWs. Morphological characterizations by scanning electron microscopy and transmission electron microscopy confirmed homogeneously aligned, smooth and clean growth of CS NWs.

References

Chaudhuri, R.G. and Paria, S. (2012), "Core/Shell Nanoparticles: Classes, Properties, Synthesis Mechanisms, Characterization, and Applications." *Chem. Rev.,* Vol. **112**, 2373.

Gapin, A.I. Ye, X.R. Aubuchon, J.F. Chen, L.H. Tang, Y. J. and Jin, S. (2006), "CoPt patterned media in anodized aluminum oxide templates." *J. Appl. Phys.,* Vol. **99**, 08G902.

Javed, K. Li, W.J. Ali, S.S. Shi, D.W. Khan, U. Riaz, S. and Han, X.F. (2015), "Enhanced exchange bias and improved ferromagnetic properties in Permalloy– $BiFe_{0.95}Co_{0.05}O_3$ core–shell nanostructures." *Sci. Repts.*, Vol. **5,**18203.

Landeros, P. Allende, S. Escrig, J. Salcedo, E. Altbir, D. and Vogel, E.E. (2007), "Reversal modes in magnetic nanotubes." *Appl. Phys. Lett.*, Vol. **90**, 102501.

Masuda, H. and Fukuda, K. (1995), "Ordered Metal Nanohole Arrays Made by a Two-Step Replication of Honeycomb Structures of Anodic Alumina." *Science,* Vol. **268**, 1466.

Maurer, T. Zighem, F. Ott, F. Chaboussant, G. and André, G. (2009), "Exchange bias in Co/CoO core-shell nanowires: Role of superparamagnetic fluctuations." *Phys. Rev. B,* Vol. **80**, 064427.

Meiklejohn, W.H. (1962), "Exchange Anisotropy—A Review." *J. Appl. Phys.,* Vol. **33**, 1328.

Moodera, J.S. and Nassar, (1999), "Spin-Tunneling In Ferromagnetic Junctions." *J. Annual Rev. Mater. Science*, Vol. **29**, 381.

Nogues, J. Schuller, I.K. (1999), "Exchange bias." *J. Magn. Magn. Mater.,* Vol. **192,** 203.

Parkin, S.S.P. Hayashi, M. and Thomas, L. (2008), "Magnetic Domain-Wall Racetrack Memory." *Science,* Vol. **320,** 190.

Shi, D.W. Chen, J. Riaz, S. Zhou, W. and Han, X.F. (2012), "Controlled nano structuring of multiphase core–shell nanowires by a template assisted electrodeposition approach." *Nanotechnology*, Vol. **23**, 305601.

Sort, J. Langlais, V. Doppiu, S. Dieny, B. Surinach, S. Munoz, J.S. Baro, M.D. Laurent, C. and Nogues, J. (2004), "Exchange bias effects in Fe nanoparticles embedded in an antiferromagnetic Cr_2O_3 matrix." *Nanotechnology,* Vol. **15,** S211.

Sun, B. Li, H. Lujun, W. and Chen, P. (2014), "Reversible resistive switching behaviors of multiferroic single-crystalline BiCoO3microribbons." *RSC Adv.*, Vol. **4**, 50102.

Zeng, H. and Sun, S. (2004), "Tailoring magnetic properties of core/shell nanoparticles." *App. Phys. Lett.,* Vol. **85**, 792.

Zeng, H. Skomski, R. Menon, L. Liu, Y. Bandyopadhyay, S. and Sellmyer, D.J. (2002), "Structure and magnetic properties of ferromagnetic nanowires in self-assembled arrays." *Phys. Rev. Lett.,* Vol. **65,** 134426.